Anomalous Quantum-Critical Scaling Corrections in Two-Dimensional Antiferromagnets

Nvsen Ma,[1,2,3] Phillip Weinberg,[3] Hui Shao,[4,3] Wenan Guo,[5,4] Dao-Xin Yao,[1,*] and Anders W. Sandvik[3,2,†]
[1]State Key Laboratory of Optoelectronic Materials and Technologies, School of Physics, Sun Yat-Sen University, Guangzhou 510275, China
[2]Beijing National Laboratory of Condensed Matter Physics and Institute of Physics, Chinese Academy of Sciences, Beijing 100190, China
[3]Department of Physics, Boston University, Boston, Massachusetts 02215, USA
[4]Beijing Computational Science Research Center, Beijing 100193, China
[5]Department of Physics, Beijing Normal University, Beijing 100084, China

(Received 4 April 2018; revised manuscript received 24 July 2018; published 12 September 2018)

We study the Néel-paramagnetic quantum phase transition in two-dimensional dimerized $S = 1/2$ Heisenberg antiferromagnets using finite-size scaling of quantum Monte Carlo data. We resolve the long-standing issue of the role of cubic interactions arising in the bond-operator representation when the dimer pattern lacks a certain symmetry. We find nonmonotonic (monotonic) size dependence in the staggered (columnar) dimerized model, where cubic interactions are (are not) present. We conclude that there is a new irrelevant field in the staggered model, but, at variance with previous claims, it is not the leading irrelevant field. The new exponent is $\omega_2 \approx 1.25$ and the prefactor of the correction $L^{-\omega_2}$ is large and comes with a different sign from that of the conventional correction with $\omega_1 \approx 0.78$. Our study highlights competing scaling corrections at quantum critical points.

DOI: 10.1103/PhysRevLett.121.117202

One of the best understood quantum phase transitions is that between Néel antiferromagnetic (AFM) and quantum paramagnetic ground states in bipartite two- and three-dimensional dimerized Heisenberg models with inter- and intradimer couplings J_1 and J_2 [1–6]. The ground state hosts AFM order when $g = J_2/J_1 \approx 1$, and there is a critical point at some model-dependent $g_c > 1$. The 3D version of this transition for $S = 1/2$ spins has an experimental realization in $TlCuCl_3$ under high pressure [7,8]. While no 2D realization exists as of yet (though the magnetic field driven transition has been realized [9]), this case has been very important for developing the framework for 2D quantum phase transitions of the Néel AFM state [10]. The field theory of the AFM-paramagnetic transition is now well developed, and efficient quantum Monte Carlo (QMC) methods can be used to study ground states of microscopic models with tens of thousands of spins [6]. Many nontrivial predictions for scaling in temperature, frequency, system size, etc., have been tested [11–16].

Despite many successes, there are still questions surrounding the 2D AFM-paramagnetic transition. A long-standing unresolved issue is differences observed in QMC calculations between two classes of dimer patterns [17–21], exemplified by the often-studied columnar dimer model (CDM) and the initially less-studied staggered dimer model (SDM), both illustrated in Fig. 1. Indications from finite-size scaling of a universality class different from the expected 3D O(3) class in the SDM [17] led to several follow-up studies [18–21]. The consensus now is that there is no new universality class, as defined by the standard critical exponents. However, because of the lack of a certain local symmetry, cubic interactions arise in the bond-operator description of the SDM, which in the renormalization group corresponds to an irrelevant field that is present neither in the CDM nor in the classical O(3) model [20]. Thus, the SDM contains an interesting quantum effect worthy of further investigations.

In this Letter we report detailed comparisons of the finite-size (L) scaling corrections of type $L^{-\omega}$ in the CDM and SDM. While previous works on judiciously chosen observables [19] and lattices with optimized aspect ratios [21] have convincingly demonstrated O(3) universality, the reasons for the unusual scaling behaviors of the SDM have never been adequately explained. In Ref. [20], QMC calculations indicated that the exponent of the leading

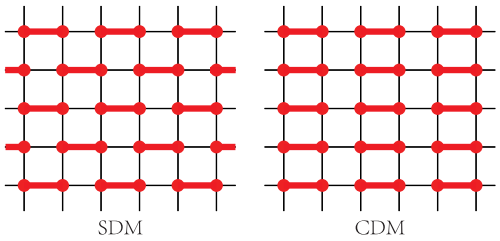

FIG. 1. The Heisenberg SDM and CDM studied in this work. Black (thinner) and red (thicker) bonds represent intra- and interdimer exchange $\mathbf{S}_i \cdot \mathbf{S}_j$, of strength (prefactor) J_1 and J_2, respectively, between $S = 1/2$ spins.

correction is smaller than in the CDM, but the value, $\omega \approx 0.6$ in the SDM [20,21] versus the conventional value $\omega \approx 0.78$ [22,23] in the O(3) model and the CDM, is not very different and cannot explain all the observed anomalous finite-size scaling properties of the SDM.

We here study $L \times L$ CDM and SDM systems of size up to $L = 256$. Focusing on the scaling corrections, we fix the leading critical exponents at their known O(3) values in our finite-size analysis, which allows us to reliably investigate also subleading corrections. In contrast to the previous studies, we demonstrate that the SDM actually does not have a smaller ω_1 than the CDM. Instead, the cubic interaction induces the next correction, which has $\omega_2 = 1.25(3)$ (where the number within parentheses here and henceforth denotes the statistical error in the preceding digit) and a large prefactor of sign different from that of the first correction. This causes nonmonotonic finite-size behaviors that were previously either not observed [19,20] or not analyzed properly [21].

QMC and fitting procedures.—We here use the standard stochastic series expansion QMC method [6,24] for $S = 1/2$ spins and set the inverse temperature β at $L/2$ (so that L/β is close to the spin-wave velocity [21]). At a quantum phase transition with dynamic exponent $z = 1$ (as is the case here), as long as $\beta \propto L$ the temperature does not appear as an independent argument in the scaling function obtained from renormalization group theory. In the case of a dimensionless quantity we have [25,26]

$$O(g, L) = f[(g - g_c)L^{1/\nu}, \lambda_1 L^{-\omega_1}, \lambda_2 L^{-\omega_2}, \ldots], \quad (1)$$

if g is sufficiently close to g_c. Here λ_i denotes the irrelevant fields, which we order such that $\omega_{i+1} > \omega_i > 0$. Useful dimensionless quantities to study in QMC calculations include the Binder ratio $R = \langle m_z^4 \rangle / \langle m_z^2 \rangle^2$, where m_z is the component of the staggered magnetization along the quantization axis, the L-normalized spin stiffness constants $L\rho_x$ and $L\rho_y$ (with x and y referring to the lattice directions), and the uniform susceptibility $L\chi_u$. We refer to Ref. [6] for technical details.

To linear order in the first irrelevant field, Eq. (1) can be written as

$$O(g, L) = f_0(\delta L^{1/\nu}) + L^{-\omega_1} f_1(\delta L^{1/\nu}), \quad (2)$$

where $\delta = g - g_c$ and f_0 and f_1 are scaling functions related to the original f. Thus, in the absence of corrections ($f_1 = 0$), a dimensionless quantity is size independent at g_c, and by expanding f_0 we see that $O(g, L)$ for different L cross each other at g_c. With the scaling correction included, the crossing points only drift toward g_c as $L \to \infty$, and for two different sizes L and $L' = rL$ one can derive simple expressions for the crossing value $g^*(L)$ and the observable $O^*(L)$ at this point [27];

$$g^*(L) = g_c + aL^{-\omega_1 - 1/\nu}, \quad (3a)$$

$$O^*(L) = O_c + bL^{-\omega_1}, \quad (3b)$$

where only a and b depend on r. We use $r = 2$ as a convenient size ratio allowing for a large number of size pairs $(L, 2L)$, with size series of the form $L = s2^n$ for a range of integers n and several choices of s. Tests with other r reveal no changes in the asymptotics.

We extract the crossings using third-order polynomial fits to ten or more data points in the neighborhood of $g_c = g^*(\infty)$, with the window $[g_{\min}, g_{\max}]$ reduced as L is increased. Such interpolations give reliable crossing points, and statistical errors are computed using bootstrapping. Examples of data with fits are shown in Fig. 2.

When fitting the crossing points $g^*(L)$ and $O^*(L)$ to their appropriate finite-size scaling forms, the same system size L can appear in two pairs, $(L, 2L)$ as well as $(L/2, L)$. There are therefore some covariance effects, which we take into account by using the full covariance matrix (computed using bootstrap analysis) in the definition of the goodness of the fit χ^2. When jointly fitting to two different quantities, we also account for the associated covariance. For the functional forms, we will go beyond the first-order expansion leading to Eqs. (3), and this will be the key to our findings and conclusions.

Finite-size scaling.—The size dependence of R crossing points is shown in Fig. 3 for both models. A striking feature is the nonmonotonic behaviors apparent for the SDM but not present for the CDM. Note here that $1/L$ on the horizontal axis refers to the smaller of the two system sizes $(L, 2L)$ used for the crossing points, and the maximums in g^* and R^* are at $2L \approx 80$. In the original discovery of the anomalous behaviors for the SDM [17], the systems were smaller and the correct asymptotic behaviors were therefore not reached.

We will first assume that only one irrelevant field is important but treat the corrections beyond the first-order expansion in $L^{-\omega_1}$, Eq. (2). Later we will argue that one

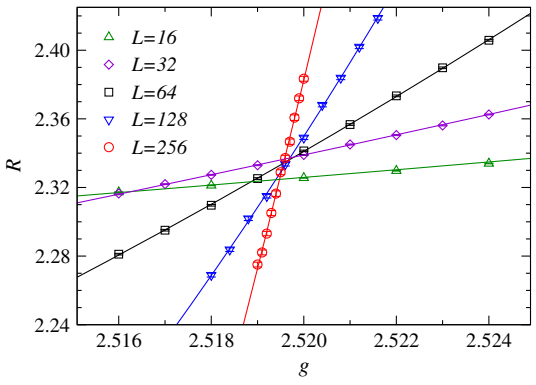

FIG. 2. Binder ratio of the SDM for several system sizes in the neighborhood of g_c. The curves are polynomial fits giving crossing points (g^*, R^*) between $(L, 2L)$ data.

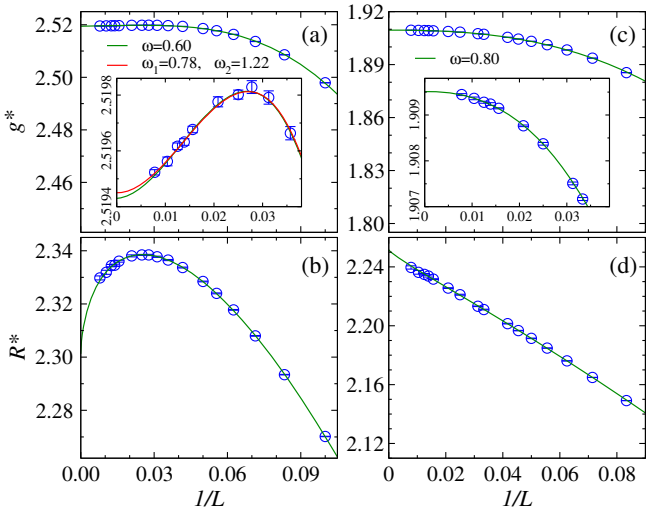

FIG. 3. Inverse system size dependence of $(L, 2L)$ crossing data for the SDM (a),(b) and the CDM (c),(d) along with joint fits (green curves) of the forms in Eqs. (4). The exponent ω is adjusted for optimal fits, giving $\omega = 0.60(4)$ for the SDM and $\omega = 0.80(2)$ for the CDM. The insets show the large system data on more detailed scales. The red curve in the inset of (a) shows a fit with only the leading terms arising from the first and second irrelevant fields, with $\omega_1 = 0.78$ fixed and $\omega_2 = 1.22(5)$ resulting from the fit; the corresponding fitting curve in (b) barely changes and is not shown.

has to include also the $L^{-\omega_2}$ term in the case of the SDM, while for the CDM ω_2 is much larger and does not have to be considered. Even with only one irrelevant field, if the associated exponent $\omega = \omega_1$ is small, the higher-order terms such as $L^{-2\omega}$ will also be important. As a guide to how far to go, we here compare the previous estimates $\omega_1 \approx 0.5$–0.6 [20,21] in the SDM with the second correction of the O(3) model, with $\omega_2 \approx 1.8$ [28], and note that several additional corrections with exponents close to 2 are expected [29]. It would then be pointless to go to higher order than 3ω in the first irrelevant field, and with $1/\nu \approx 1.4$ we also do not include mixed corrections with ω and $1/\nu$. Thus, for the SDM we use

$$g^*(L) = g_c + L^{-1/\nu}(a_1 L^{-\omega} + a_2 L^{-2\omega} + a_3 L^{-3\omega}), \tag{4a}$$

$$R^*(L) = R_c + b_1 L^{-\omega} + b_2 L^{-2\omega} + b_3 L^{-3\omega}, \tag{4b}$$

and exclude small systems until good fits are obtained. For the CDM, with $\omega_1 = 0.78$, by the above arguments we stop at 2ω.

The fitting coefficients a_i and b_i in Eq. (4) are not fully independent of each other but are related because they originate from the same scaling function, Eq. (1). We do not write down the relationships here but fully take them into account in joint fits of the g^* and O^* data. These nonlinear fits are quite demanding, and we make use of a slow but reliable stochastic approach [30]. The stability of the fits is greatly aided by fixing $1/\nu$ to its known 3D O(3) value, 1.406 [23]. The resulting curves are shown in Fig. 3. Here, as in all cases below, all data points shown in the figure were included in the fits (with smaller sizes excluded until the fits have acceptable χ^2 values).

For the CDM, our result for the critical coupling is $g_c = 1.90951(1)$. The value is consistent with the best previous results, $g_c = 1.90948(4)$ [6] and $g_c = 1.90947(3)$ [21], but with reduced statistical error. For the correction, we obtain $\omega = 0.80(2)$, which agrees with the O(3) value $\omega_1 = 0.782(13)$ [23].

For the SDM we obtain $g_c = 2.51943(1)$. Using rectangular lattices with optimized aspect ratio, a compatible result, $g_c = 2.51941(2)$, was obtained [21]. For the correction we obtain $\omega = 0.60(4)$, which is clearly smaller than the known O(3) value cited above but in good agreement with the values presented in Refs. [20,21].

Although R_c is universal in the sense that it does not depend on the microstructure of lattice and details of the interactions, it does depend on boundary conditions [31,32] and aspect ratios [21]. The CDM and SDM have different critical spin-wave velocities and, therefore, effectively different time-space aspect ratios even though β/L is the same. This explains the different R_c values in Fig. 3; see also Supplemental Material [33].

By also analyzing the spin stiffness and the uniform susceptibility in the manner described above, we obtain the results summarized in Table I. The results for the CDM consistently reproduce the known O(3) value of ω_1, while in the case of the SDM the different quantities produce a wide range of results. The latter suggests that ω may not be the true smallest correction exponent in the case of the SDM, but, as also pointed out in Ref. [20], should be regarded as an "effective exponent" influenced by neglected further corrections. The inability of a single irrelevant field to describe the data is actually not unexpected within the scenario of irrelevant cubic interactions [20], because the standard leading correction with $\omega_1 \approx 0.78$ should still be present and may produce various "effective" scaling behaviors over a limited range of system sizes when combined with the cubic perturbation. Thus, a reliable analysis of the SDM should require at least ω_1 and ω_2.

TABLE I. Results for the critical point and correction exponent obtained from fits of various dimensionless quantities to scaling forms analogous to Eqs. (4), keeping corrections up to 3ω for the SDM and 2ω for the CDM.

	SDM		CDM	
	ω	g_c	ω	g_c
$L\rho_x$	0.88(2)	2.51946(2)	0.77(3)	1.90953(2)
$L\rho_y$	0.39(5)	2.51942(3)	0.77(4)	1.90957(2)
$L\chi_u$	0.68(6)	2.51945(2)	0.78(3)	1.90956(3)
R	0.60(4)	2.51943(1)	0.80(2)	1.90951(1)

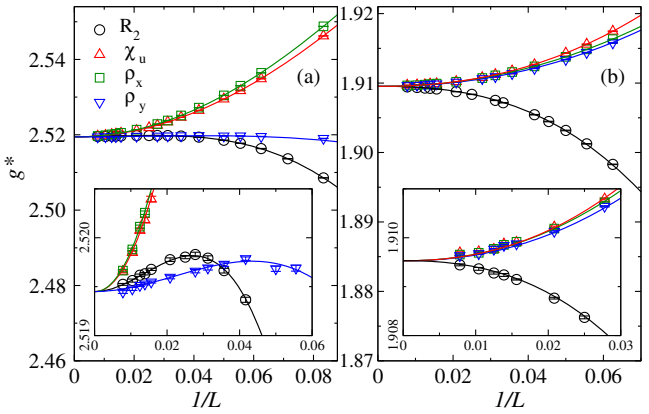

FIG. 4. Joint fits of crossing data for several quantities where $g^*(\infty) = g_c$ is fixed to a common value and two corrections are used to first order, with $\omega_1 = 0.78$ and $1/\nu = 1.406$. The insets zoom in on the data for the larger system sizes. For the SDM (a), the fit delivers $g_c(\infty) = 2.51945(1)$ and $\omega_2 = 1.30(7)$, 1.3(1), 1.2(1), and 1.0(2) from R, $L\chi_u$, $L\rho_x$, and $L\rho_y$, correspondingly. In the CDM fits (b), $2\omega_1 = 1.56$ was used in place of ω_2 and $g_c = 1.90956(2)$.

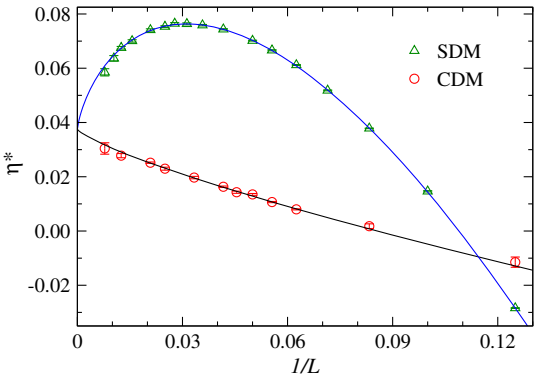

FIG. 5. Size dependence of the exponent η as defined in Eq. (6). The known infinite-size value $\eta = 0.0375$ is fixed in the fits (curves). The CDM data are fitted with only the first correction term in Eq. (7), with $\omega_1 = 0.78$ fixed. In the SDM fit, $\omega_1 = 0.78$ is also fixed and the second exponent $\omega_2 = 1.29(5)$ is the result of the fit.

We can generalize Eqs. (4) to two correction exponents, ω_1 and ω_2, but in that case it is difficult to determine both of them with sufficient precision. However, since the standard leading correction should still be present [20], we now also fix $\omega_1 = 0.78$ and only treat ω_2 as a free parameter. It is then sufficient to go to linear order in the corrections and yet obtain fully acceptable fits. We obtain $g_c = 2.51945(1)$ and $\omega_2 = 1.22(5)$ for the SDM. The new fitted curve is shown in the inset of Fig. 3(a). The estimate of g_c is a bit higher than the previous value from R^*, but the difference is not statistically significant.

The key result here is clearly that ω_2 comes out larger than the leading O(3) exponent. It is, however, significantly smaller than the expected second irrelevant O(3) exponent with value ≈ 1.8 [28,29], and it is also less than $2\omega_1$. The new correction should therefore be due to the cubic interactions [20] in the low-energy theory of the SDM. To test the stability of ω_2 across different quantities, we also used a slightly different procedure of fitting only to g^* (instead of the joint fit with R^*) and requiring the same $L \to \infty$ value of g_c for all the quantities considered. We still also fix $1/\nu = 1.406$ and $\omega_1 = 0.78$ but keep ω_2 free for all individual quantities. The SDM data with fits are displayed in Fig. 4(a), with the resulting g_c and ω_2 estimates listed in the caption. The fits are statistically good and all four ω_2 estimates are consistent with the value obtained above. In the case of the CDM, shown Fig. 4(b), we follow the same procedures but replace ω_2 by $2\omega_1$, and there is no free exponent. This fit is only of marginally acceptable statistical quality even when starting the fits from $L = 16$, indicating some effects still of the higher-order terms that were included in Fig. 3(b). We therefore keep the value from R in Table I as our best g_c estimate for this model.

To further ascertain our conclusions about the SDM, we also consider the squared order parameter itself. Having determined a precise estimate of g_c, we study the scaling of $\langle m^2 \rangle$ at this point, where we expect

$$\langle m^2 \rangle_c \propto L^{-(1+\eta)}(1 + b_1 L^{-\omega_1} + b_2 L^{-\omega_2} + \cdots). \quad (5)$$

We can then define a size-dependent exponent as

$$\eta^*(L) = \ln[\langle m^2(L) \rangle_c / \langle m^2(2L) \rangle_c] / \ln(2) - 1, \quad (6)$$

which should scale as

$$\eta^*(L) = \eta + c_1 L^{-\omega_1} + c_2 L^{-\omega_2} + \cdots. \quad (7)$$

To test this form and extract ω_2, we use the known value $\eta = 0.0375(5)$ [23] and fix $\omega_1 = 0.78$. As shown in Fig. 5, the form fits the data very well and gives $\omega_2 = 1.29(5)$. Here, one can again see how access to only system sizes less than $L = 80$ could easily lead to the wrong conclusion. A fit with two adjustable exponents gives $\omega_1 = 0.77(6)$ and $\omega_2 = 1.31(7)$, perfectly consistent with the fit with ω_1 fixed. In the case of the CDM, also shown in Fig. 5, we find that the data are well described with a single correction with the known value of the exponent.

Conclusions.—We have analyzed the SDM under the scenario [20] of an O(3) quantum phase transition with an additional irrelevant perturbation that is absent in the CDM. Our results are consistent with this picture and demand a new scaling correction with exponent $\omega_2 \approx 1.25$ that is larger than the also present conventional 3D O(3) exponent $\omega_1 \approx 0.78$ but smaller than the next known O(3) exponent. Thus, the cubic interactions in the low-energy theory are formally more irrelevant than previously believed [20,21],

but their effects are important in finite-size scaling of many quantities because of their different signs and larger prefactors of the correction terms (4 times larger than the factor of the leading correction in the case of the order parameter), thus giving rise to nonmonotonic behaviors.

In addition to resolving the role of the cubic interactions in the class of models represented by the SDM, our study also serves as an example of finite-size behaviors that may at first sight appear puzzling but can be understood once the possibility of competing scaling corrections is recognized. Nonmonotonic scaling has also been observed at the deconfined quantum phase transitions, which has complicated efforts to extract the critical point and exponents [34].

We would like to thank Ning Su, Stefan Wessel, and Matthias Vojta for useful discussions. The work of N. M. and D.-X. Y. was supported by Grants No. NKRDPC-2017YFA0206203, No. NKRDPC-2018YFA0306001, No. NSFC-11574404, No. NSFC-11275279, No. NSFG-2015A030313176, and the Leading Talent Program of Guangdong Special Projects. H. S. was supported by the China Postdoctoral Science Foundation under Grants No. 2016M600034 and No. 2017T100031. W. G. was supported by NSFC under Grants No. 11775021 and No. 11734002. A. W. S was supported by the NSF under Grant No. DMR-1710170 and by a Simons Investigator Award. Some of the calculations were carried out on Boston University's Shared Computing Cluster.

*yaodaox@mail.sysu.edu.cn
†sandvik@bu.edu

[1] S. Chakravarty, B. I. Halperin, and D. R. Nelson, Phys. Rev. Lett. **60**, 1057 (1988).
[2] R. R. P. Singh, M. P. Gelfand, and D. A. Huse, Phys. Rev. Lett. **61**, 2484 (1988).
[3] A. J. Millis and H. Monien, Phys. Rev. Lett. **70**, 2810 (1993).
[4] A. V. Chubukov, S. Sachdev, and J. Ye, Phys. Rev. B **49**, 11919 (1994).
[5] S. Sachdev, *Quantum Phase Transition*, 2nd ed. (Cambridge University Press, Cambridge, England, 2011).
[6] A. W. Sandvik, AIP Conf. Proc. **1297**, 135 (2010).
[7] P. Merchant, B. Normand, K. W. Kramer, M. Boehm, D. F. McMorrow, and C. Rüegg, Nat. Phys. **10**, 373 (2014).
[8] Y. Q. Qin, B. Normand, A. W. Sandvik, and Z. Y. Meng, Phys. Rev. B **92**, 214401 (2015).
[9] T. Giamarchi, C. Rüegg, and O. Tchernyshyov, Nat. Phys. **4**, 198 (2008).
[10] S. Sachdev, Nat. Phys. **4**, 173 (2008).
[11] A. W. Sandvik and D. J. Scalapino, Phys. Rev. Lett. **72**, 2777 (1994).
[12] M. Troyer, H. Kontani, and K. Ueda, Phys. Rev. Lett. **76**, 3822 (1996).
[13] M. Matsumoto, C. Yasuda, S. Todo, and H. Takayama, Phys. Rev. B **65**, 014407 (2001).
[14] L. Wang, K. S. D. Beach, and A. W. Sandvik, Phys. Rev. B **73**, 014431 (2006).
[15] A. Sen, H. Suwa, and A. W. Sandvik, Phys. Rev. B **92**, 195145 (2015).
[16] M. Lohöfer, T. Coletta, D. G. Joshi, F. F. Assaad, M.Vojta, S. Wessel, and F. Mila, Phys. Rev. B **92**, 245137 (2015).
[17] S. Wenzel, L. Bogacz, and W. Janke, Phys. Rev. Lett. **101**, 127202 (2008).
[18] F.-J. Jiang and U. Gerber, J. Stat. Mech. (2009) P09016.
[19] F.-J. Jiang, Phys. Rev. B **85**, 014414 (2012).
[20] L. Fritz, R. L. Doretto, S. Wessel, S. Wenzel, S. Burdin, and M. Vojta, Phys. Rev. B **83**, 174416 (2011).
[21] S. Yasuda and S. Todo, Phys. Rev. E **88**, 061301(R) (2013).
[22] R. Guida and J. Zinn-Justin, J. Phys. A **31**, 8103 (1998).
[23] M. Campostrini, M. Hasenbusch, A. Pelissetto, P. Rossi, and E. Vicari, Phys. Rev. B **65**, 144520 (2002).
[24] A. W. Sandvik, Phys. Rev. B **59**, R14157 (1999).
[25] M. N. Barber, in *Phase Transitions and Critical Phenomena*, edited by C. Domb and J. L. Lebowitz (Academic Press, New York, 1983), Vol. 8.
[26] M. Campostrini, A. Pelissetto, and E. Vicari, Phys. Rev. B **89**, 094516 (2014).
[27] J. M. Luck, Phys. Rev. B **31**, 3069 (1985).
[28] K. E. Newman and E. K. Riedel, Phys. Rev. B **30**, 6615 (1984).
[29] M. Hasenbusch, J. Phys. A **34**, 8221 (2001).
[30] C. Liu, L. Wang, A. W. Sandvik, Y.-C. Su, and Y.-J. Kao, Phys. Rev. B **82**, 060410(R) (2010).
[31] G. Kamienartz and H. W. J. Blöte, J. Phys. A **26**, 201 (1993).
[32] W. Selke, J. Stat. Mech. (2007) P04008.
[33] See Supplemental Material at http://link.aps.org/supplemental/10.1103/PhysRevLett.121.117202 for the dependence of R on the space-time aspect ratio.
[34] H. Shao, W. Guo, and A. W. Sandvik, Science **352**, 213 (2016).